Article

Cell Metabolism

Calcineurin Links Mitochondrial Elongation with Energy Metabolism

Graphical Abstract

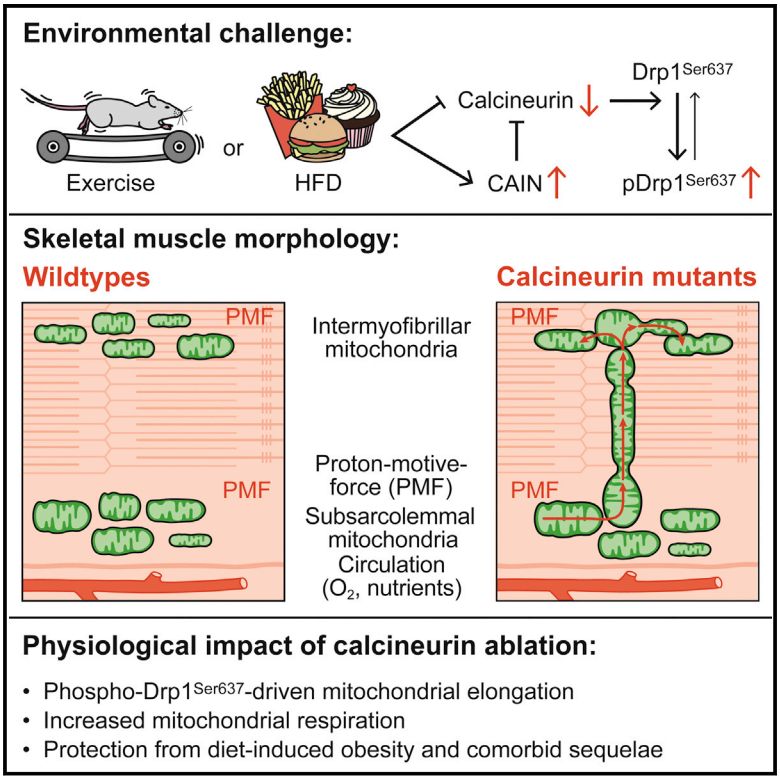

Highlights

- Fly mutants for calcineurin (Ppp3) display low body weight and high respiration
- Global and skeletal muscle-specific Ppp3 KO mice are protected from obesity
- Ppp3 ablation enhances Drp1^{S637}-hyperphosphorylation and mitochondrial respiration
- Ppp3 KO mice display elongated mitochondria but attenuated exercise capacity

Authors

Paul T. Pfluger, Dhiraj G. Kabra, Michaela Aichler, ..., Maria De Luca, Jeffery D. Molkentin, Matthias H. Tschöp

Correspondence

matthias.tschoep@helmholtz-muenchen.de

In Brief

Pfluger et al. reveal an evolutionary conserved role for the phosphatase calcineurin in the adaptive regulation of body weight and energy homeostasis in flies and mice. Calcineurin ablation from skeletal muscle enhances Drp1^{Ser637}-hyperphosphorylation, increases mitochondrial elongation and respiration, and protects from diet-induced obesity while attenuating exercise capacity.

Pfluger et al., 2015, Cell Metabolism 22, 838–850
November 3, 2015 ©2015 Elsevier Inc.
http://dx.doi.org/10.1016/j.cmet.2015.08.022

CellPress

Cell Metabolism
Article

Calcineurin Links Mitochondrial Elongation with Energy Metabolism

Paul T. Pfluger,[1] Dhiraj G. Kabra,[1] Michaela Aichler,[2] Sonja C. Schriever,[1] Katrin Pfuhlmann,[1] Verónica Casquero García,[1] Maarit Lehti,[3] Jon Weber,[4] Maria Kutschke,[1] Jan Rozman,[1,5] John W. Elrod,[6] Andrea L. Hevener,[7] Annette Feuchtinger,[2] Martin Hrabě de Angelis,[1,5] Axel Walch,[2] Stephanie M. Rollmann,[8] Bruce J. Aronow,[9] Timo D. Müller,[1] Diego Perez-Tilve,[4] Martin Jastroch,[1] Maria De Luca,[10] Jeffery D. Molkentin,[11,12] and Matthias H. Tschöp[1,13,*]

[1]Helmholtz Diabetes Center
[2]Research Unit Analytical Pathology
Helmholtz Zentrum München, 85764 Neuherberg, Germany
[3]LIKES Research Center for Sport and Health Sciences, 40720 Jyväskylä, Finland
[4]Department of Internal Medicine, Division of Endocrinology, Metabolic Diseases Institute, University of Cincinnati, Cincinnati, OH 45237, USA
[5]German Mouse Clinic, Institute of Experimental Genetics, Helmholtz-Zentrum München, 85764 Neuherberg, Germany
[6]Department of Pharmacology, Center for Translational Medicine, Temple University School of Medicine, Philadelphia, PA 19140, USA
[7]Division of Endocrinology, Diabetes, and Hypertension, David Geffen School of Medicine, University of California, Los Angeles, Los Angeles, CA 90095, USA
[8]Department of Biological Sciences, University of Cincinnati, Cincinnati, OH 45221, USA
[9]Division of Biomedical Informatics, Cincinnati Children's Hospital Medical Center, Cincinnati, OH 45229, USA
[10]Department of Nutrition Sciences, University of Alabama at Birmingham, Birmingham, AL 35294, USA
[11]Howard Hughes Medical Institute
[12]Department of Pediatrics
Cincinnati Children's Hospital Medical Center, Cincinnati, OH 45229, USA
[13]Division of Metabolic Diseases, Technische Universität München, 80333 Munich, Germany
*Correspondence: matthias.tschoep@helmholtz-muenchen.de
http://dx.doi.org/10.1016/j.cmet.2015.08.022

SUMMARY

Canonical *protein phosphatase 3*/calcineurin signaling is central to numerous physiological processes. Here we provide evidence that calcineurin plays a pivotal role in controlling systemic energy and body weight homeostasis. Knockdown of calcineurin in *Drosophila melanogaster* led to a decrease in body weight and energy stores, and increased energy expenditure. In mice, global deficiency of catalytic subunit *Ppp3cb*, and tissue-specific ablation of regulatory subunit *Ppp3r1* from skeletal muscle, but not adipose tissue or liver, led to protection from high-fat-diet-induced obesity and comorbid sequelæ. Ser637 hyperphosphorylation of dynamin-related protein 1 (Drp1) in skeletal muscle of calcineurin-deficient mice was associated with mitochondrial elongation into power-cable-shaped filaments and increased mitochondrial respiration, but also with attenuated exercise performance. Our data suggest that calcineurin acts as highly conserved pivot for the adaptive metabolic responses to environmental changes such as high-fat, high-sugar diets or exercise.

INTRODUCTION

The homeostatic control of energy metabolism includes multiple organs and pathways that sense and transduce environmental stimuli into adaptive responses. Mitochondria play an integral role in this rapid adaptation to varying nutrient substrates and bioenergetic demand by forming interwebbed mitochondrial networks, which are reshaped dynamically by fusion and fission events (Liesa and Shirihai, 2013). Mitochondrial fusion, governed by enzymes such as mitofusin 1/2 and optic atrophy factor 1 (OPA1), mitigates cellular stress by distributing damaged mitochondrial content over a wider compartment. Fragmentation of mitochondria by fission, mainly catalyzed by the enzyme dynamin-related protein 1 (Drp1), helps to dispose damaged mitochondria via mitophagy (Liesa et al., 2009). While the complete lack of fusion or fission was linked to severe neurodegenerative diseases such as Parkinson's disease or Alzheimer's disease (Reddy et al., 2011), shifts in balance between fusion and fission are an important adaptive process required to retain mitochondrial flexibility and health upon changes to our environment (Dietrich et al., 2010; Schneeberger et al., 2013).

To date, little is known about the exact molecular mechanisms that control mitochondrial dynamics elicited by environmental stimuli. Calcineurin (Protein Phosphatase 3, *Ppp3*), a ubiquitously expressed calcium-sensitive serine-threonine phosphatase comprised of a 61 kD calmodulin-binding catalytical subunit A (gene name, *Ppp3c*) and 19 kD Ca^{2+}-binding regulatory subunit B (gene name, *Ppp3r*) (Klee et al., 1979), is known to dephosphorylate and thereby inhibit Drp1 activity (Cereghetti et al., 2008; Cribbs and Strack, 2007). Three genes are encoding the catalytic subunit A: *Ppp3ca* (isoform α), *Ppp3cb* (isoform β), or *Ppp3cc* (isoform γ), with *Ppp3ca* and *Ppp3c* displaying partially overlapping expression patterns and functions (Rusnak and Mertz, 2000). For the regulatory subunit B, two genes have been described (*Ppp3r1* and *Ppp3r2*), but *Ppp3r2* expression

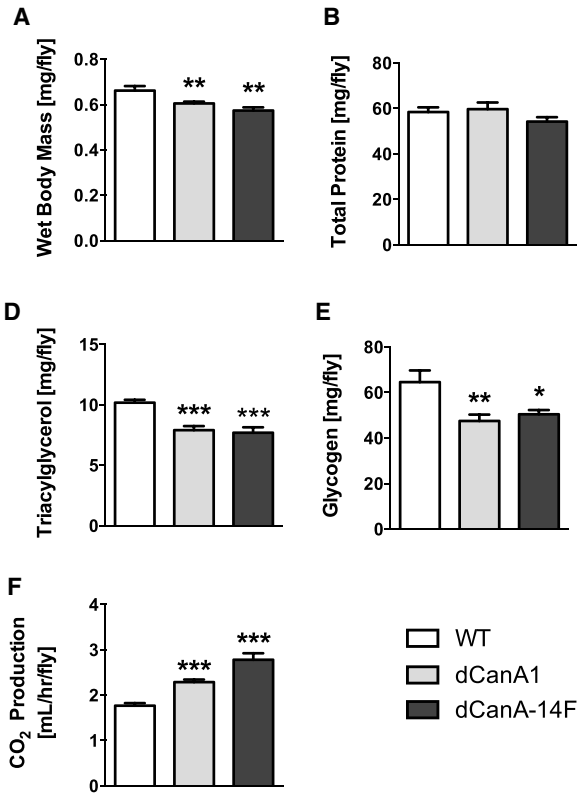

Figure 1. Metabolic Traits in Male *Drosophila melanogaster* Calcineurin Mutants

(A and B) Wet body mass and protein content in isogenic w^{1118} wild-type controls (WT) and fly mutants with piggyBac transposon mutations of *dCanA1* or *dCanA-14F*.

(C) Microarrays of RNA extracted from fly thoraxes of WT and calcineurin mutant flies.

(D and E) Whole-body triglyceride and glycogen levels of WT and calcineurin mutant flies.

(F) CO_2 production in WT and calcineurin mutant flies was assessed by indirect calorimetry.

Means ± SEM. n = 4–6 with 10–50 flies per replicate, as described in the experimental procedures. *p < 0.05, **p < 0.01, ***p < 0.001.

seems to be confined to testes (Liu et al., 2005). Calcineurin is activated by an influx of intracellular calcium, and represents a key-signaling node that conveys environmental stimuli into an adaptive response in multiple tissues and organs.

We pursued the hypothesis that calcineurin may act as an environmentally controlled signaling nexus for mitochondrial dynamics that exerts tissue-specific effects on the control of body weight and energy homeostasis. Using piggyBac transposon fly mutants, mice with global deficiency of *Ppp3cb*, and mice with skeletal muscle-specific ablation of *Ppp3r1*, we provide evidence that calcineurin plays a highly conserved role in environmentally induced and Drp1-mediated mitochondrial fusion, mitochondrial oxidation, and the regulation of energy metabolism and body weight.

RESULTS

Adult Calcineurin piggyBac Mutant Flies Exhibit Increased Metabolic Rate and Decreased Body Weight

PiggyBac transposon mutants for the *Drosophila* calcineurin genes *calcineurin A1* (*dCanA1*) and *calcineurin A14F* (*dCanA14F*) displayed decreased body weights compared to WT controls (Figure 1A). Whole-body protein levels were unchanged, thereby excluding growth retardation (Figure 1B). Next, we isolated RNA from the thorax of flies and utilized whole tiling gene arrays to reveal distinctly deregulated gene patterns that appeared in both mutants as compared to the WT controls (heatmap; Figure 1C; see Table S1 available online; GEO series identifier GSE71701). Gene enrichment analyses did not suggest overt developmental deficits in our calcineurin mutant flies. Instead, there was a significant overrepresentation of metabolic pathways with multiple genes being involved in mitochondrial function, increased transmembrane transporter activity, and enhanced oxidative substrate utilization in both calcineurin mutants, pointing to an important role of calcineurin in the regulation of energy homeostasis and storage of calories (Table S1). Accordingly, we observed a decrease in whole-body triacylglycerol and glycogen levels in both mutants compared to WT controls (Figures 1D and 1E). Glycerol levels remained unchanged (data not shown). Last, to reveal whether the decreased energy storage could be a result of enhanced energy expenditure, we subjected the WT flies and calcineurin mutants to indirect calorimetry analyses. We observed increased CO_2 production in both mutants compared to WT controls, indicating enhanced metabolic rates in calcineurin mutant flies (Figure 1F).

Pharmacological Inhibition of Calcineurin Activity in Mice Reduces Diet-Induced Obesity

Sequence comparisons reveal remarkable homologies between Ppp3 isoforms from different species (Jiang and Cyert, 1999). *D. melanogaster CanA1*, *Mus musculus Ppp3cb*, and human *Ppp3cb* share 55% homology. Accordingly, we aimed to evaluate whether the observed role of calcineurin in *Drosophila* could also be replicated in a mammalian system. We first injected the calcineurin inhibitor FK-506 (1 mg/kg) daily for 7 days into diet-induced obese (DIO) mice and observed a clear reduction in body weight (Figure 2A) and fat mass (vehicle, −0.14% ± 1.84% fat mass loss versus FK-506, −9.8% ± 0.98% fat mass loss; p = 0.00037). However, since FK506 has also been shown to inhibit calcineurin-independent pathways (Klettner and Herdegen, 2003), we next employed a genetic model of calcineurin deficiency.

Global Genetic Disruption of Calcineurin Increases Energy Expenditure and Protects from Diet-Induced Obesity

Global ablation of the regulatory subunit *Ppp3r1* evokes a nearly complete loss of calcineurin activity in mice, leading to

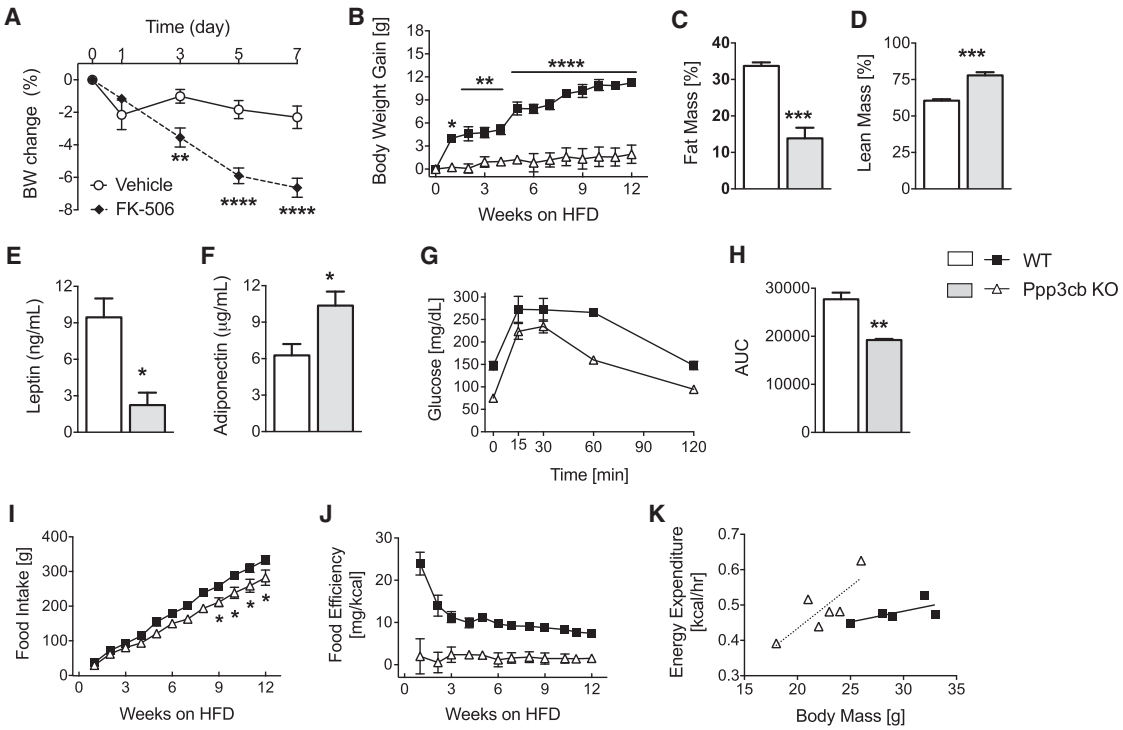

Figure 2. Global Reduction of Calcineurin Activity Improves Body Weight and Energy Homeostasis in Male Mice

(A) Body weight change in diet-induced obese C57Bl6J mice after daily subcutaneous injections of FK-506 (1 mg/kg) (n = 8).

(B–F) Genetic ablation of *Ppp3cb* leads to full protection from high-fat-diet (HFD)-induced obesity, as revealed by decreased body weight gain (B) and fat mass (C), an increase in lean mass (D), decreased plasma leptin (E), and increased plasma adiponectin levels (F) compared to HFD-fed WT mice (n = 3–4).

(G and H) Glucose tolerance test in HFD-fed Ppp3cb WT and KO mice (n = 3–4).

(I and J) Food ingestion and food efficiency in HFD-fed Ppp3cb WT and KO mice (n = 3–4).

(K) Energy expenditure of HFD-fed Ppp3cb WT and KO mice (n = 5–6) in relation to body weight.

Means ± SEM. *p < 0.05, **p < 0.01, ***p < 0.001, ****p < 0.0001.

embryonic lethality. In contrast, full ablation of the catalytic subunit *Ppp3cb* can be partially compensated by the remaining two isozymes (*Ppp3ca* and *Ppp3cc*), resulting in viable offspring. We thus decided to utilize global Ppp3cb-deficient mice with attenuated but functional calcineurin signaling (Bueno et al., 2002a).

Ppp3cb KO mice were viable and fertile, and displayed similar food intake but significantly decreased body weight and fat mass on a standardized chow diet compared to WT controls. Plasma levels of leptin, adiponectin, and FFA were decreased in Ppp3cb KO mice (Table S2). When exposed to HFD, global Ppp3cb KO mice displayed a complete protection from DIO (Figure 2B), lacking any increase in fat mass (Figure 2C) compared to the relative increase in lean mass (Figure 2D). The lean phenotype of HFD-fed Ppp3cb KO mice was accompanied by decreased circulating leptin and increased adiponectin levels (Figures 2E and 2F), and improved glucose tolerance (Figures 2G and 2H). Additional glucose challenge tests in weight-matched Ppp3cb WT and KO mice after 3 weeks of HFD feeding corroborated the decreased basal glucose levels but revealed unchanged basal and stimulated insulin secretion (Figure S1A). Food intake (two-way ANOVA, p = 0.05; Figure 2I) was slightly lower in HFD-fed Ppp3cb KO mice; yet, when normalized to body weight, the Ppp3cb KO mice displayed significantly increased food intake relative to WT controls (two-way ANOVA, p = 0.0006; Figure S1B). Notably, food efficiency, i.e., the ability of mice to translate ingested calories into body weight gain, was severely decreased in Ppp3cb KO mice (two-way ANOVA, p = 0.0009; Figure 2J), suggesting an increased metabolic rate. Such increased energy expenditure in Ppp3cb KO compared to WT mice (Figure 2K; F = 28.623, p = 0.001, n = 5–6) was revealed by indirect calorimetry with body weight as predictive covariate (F = 7.171, p = 0.028) in the ANCOVA.

In a previous report, chow-fed *Ppp3cb*-deficient mice displayed a decrease in body weight but in contrast to our studies also exhibited glucose intolerance and hyperlipidemia due to increased adipose tissue lipolysis (Suk et al., 2013). To identify potential reasons for these discrepant findings, we generated conditional KO mice with complete and specific ablation of calcineurin activity in adipose tissue.

Adipocyte-Specific Ablation of Calcineurin Does Not Protect from HFD-Induced Body Adiposity

On chow diet, Ppp3r1^{AdipoCre} KO mice displayed unchanged body weight and fat mass (Figures S2A and S2B), and indirect calorimetry revealed no overt metabolic changes in food intake, energy expenditure, locomotor activity, or respiratory quotient

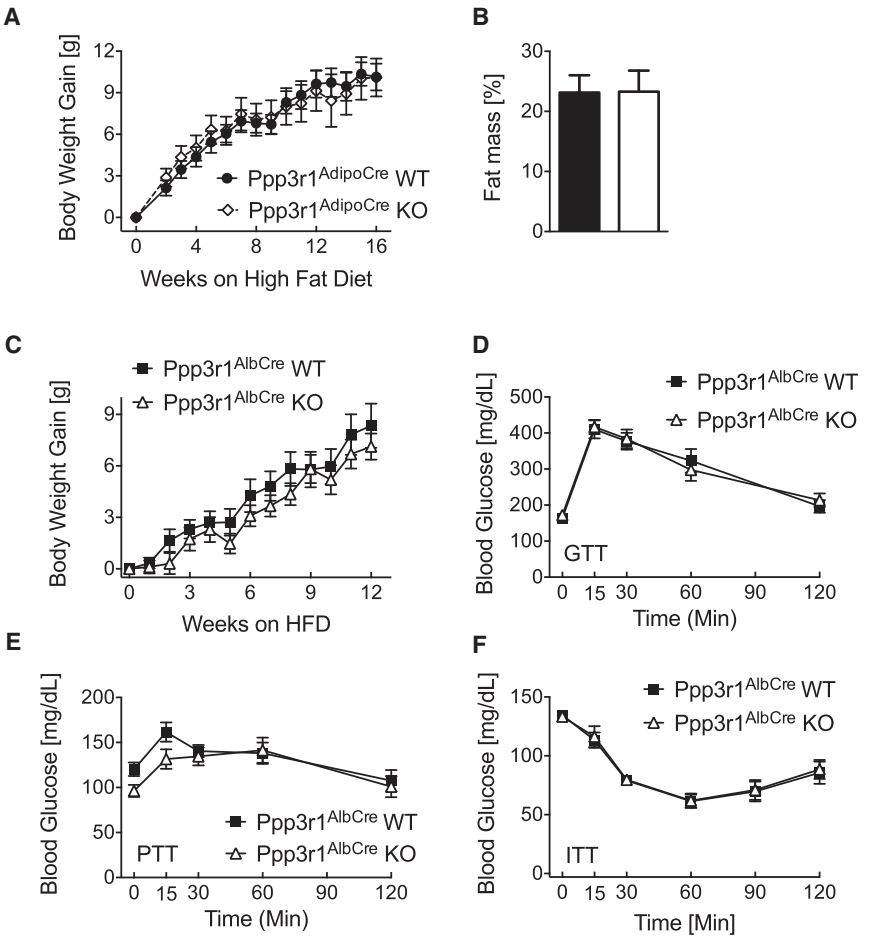

Figure 3. Adipose Tissue and Liver-Specific Ablation of *Ppp3r1* Have No Impact on Body Adiposity and Glucose Homeostasis

(A and B) Body weight gain (A) and fat mass (B) in male mice with adipose tissue-specific ablation of *Ppp3r1* (n = 7–10).

(C) Body weight gain after ablation of *Ppp3r1* from liver (n = 10).

(D and E). Male Ppp3r1^{AlbCre} WT and KO mice (n = 10) reveal similar glucose excursions in glucose (D, GTT), insulin (E, ITT), or pyruvate (F, PTT) tolerance tests.

Means ± SEM.

(Figures S2C–S2F). When exposed to HFD, Ppp3r1^{AdipoCre} KO mice developed DIO and glucose intolerance similar to HFD-fed WT littermates, as revealed by similar body weight gain (Figure 3A), fat pad weights (Figure S2G), and fat mass (Figure 3B), as well as glucose excursions (Figure S2H) and area under the curve values in a GTT (Figure S2I). Accordingly, our data do not suggest a role for calcineurin in brown or white fat lipolysis, adipose tissue thermogenesis, or adipogenesis.

Liver-Specific Ablation of Calcineurin Does Not Affect Body Weight or Glucose Homeostasis

Next, we ablated full calcineurin activity from hepatocytes by crossing albumin-Cre mice to Ppp3r1$^{fl/fl}$ mutants. Ppp3r1^{AlbCre} KO mice were fertile and viable, but displayed no changes in systemic energy and glucose homeostasis compared to WT littermates. Specifically, Ppp3r1^{AlbCre} KO mice revealed unchanged body weight, fat mass, and lean mass on chow diet (Figures S2J–S2L), and a similar propensity toward obesity on HFD (Figure 3C). Further, hepatic ablation of calcineurin did not affect systemic glucose, pyruvate, or insulin tolerance even after prolonged HFD exposure, compared to Ppp3r1^{AlbCre} WT mice (Figures 3D–3F). The latter was unexpected in light of earlier studies suggesting that calcineurin might be a regulator of hepatic gluconeogenesis in fasting and diabetes via dephosphorylation of CREB coactivator CRTC2 in response to glucagon (Wang et al., 2012). Nevertheless, recent studies questioned the requirement for hepatocytic CREB in the maintenance of glucose homeostasis (Lee et al., 2014), which would explain our finding of unabated glucose, pyruvate, and insulin tolerance in liver-specific Ppp3r1 KO mice.

Skeletal-Muscle-Specific Ablation of Calcineurin Protects from Diet-Induced Obesity and Its Metabolic Sequelæ

We evaluated whether the enhanced metabolic rate in global Ppp3cb KO mice functionally resulted from decreased calcineurin activity in skeletal muscle by crossing myosin-light chain-Cre (MlcCre) mice to Ppp3r1$^{fl/fl}$ mice. Specificity of Mlc1f-driven Cre recombination for skeletal muscle was verified in additional crosses of MlcCre mice with a double fluorescent Cre reporter line (Figure S3A). Protection from DIO in muscle-specific Ppp3r1^{MlcCre} KO mice (Figure 4A) was accompanied by significantly reduced fat mass and increased lean mass (Figures 4B and 4C) compared to HFD-fed WT mice. We found no differences in the metabolic phenotype of chow-fed Ppp3r1^{MlcCre} WT and KO mice (Figures S3B–S3I). We observed a strong trend ($p = 0.07$) toward decreased serum leptin levels in HFD-fed Ppp3r1^{MlcCre} KO mice (1,028 ± 319.2 ng/ml) compared to WT controls (3,932 ± 1187 ng/ml). Food intake in HFD-fed Ppp3r1^{MlcCre} KO mice appeared to be slightly decreased compared to WT controls (Figure 4D) but turned out to be similar when normalized to body weight (Figure S3J). Ppp3r1^{MlcCre} WT and KO mice displayed similar energy expenditure (ANCOVA; n = 11; genotype, $F = 1.924$, $p = 0.181$; predictive covariate body weight, $F = 32.107$, $p = 0.0001$; Figure 4E). Normalization to the metabolic mass appeared to increase dark phase energy expenditure in HFD-fed Ppp3r1^{MlcCre} KO mice compared to WT controls (Figure S3K), but such normalization may not be adequate to account for the impact of body composition changes on energy expenditure (Tschöp et al., 2012). Assimilation efficiency was similar in HFD-fed Ppp3r1^{MlcCre} WT and KO mice (Figure 4F), indicating normal gastrointestinal handling of the food consumed. However, while HFD-fed WT mice efficiently

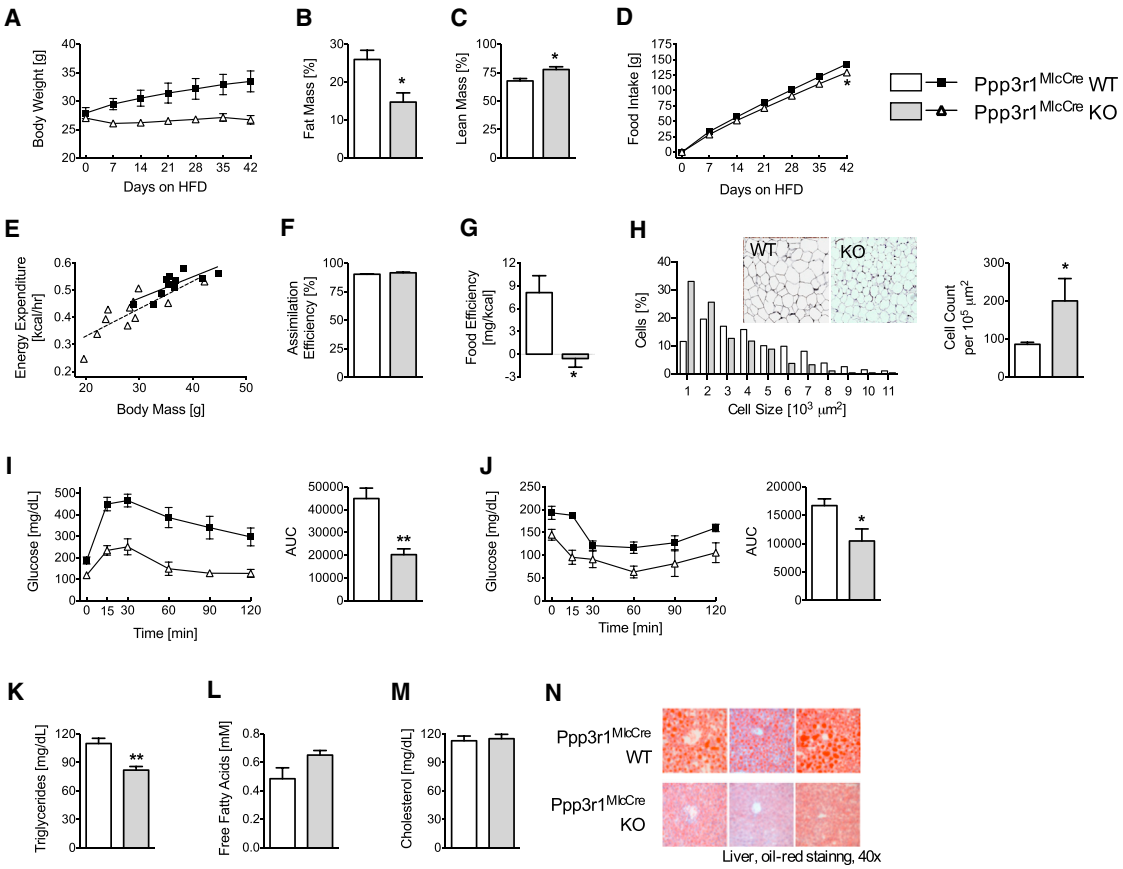

Figure 4. Skeletal Muscle-Specific Ablation of *Ppp3r1* Protects from Diet-Induced Obesity and Its Sequelæ

(A–C) Body weight gain (A) and relative fat (B) and lean mass (C) after 6 weeks of HFD exposure in male skeletal muscle-specific *Ppp3r1* WT and KO mice (n = 5).

(D–G) Food intake (D, n = 5), energy expenditure (E, n = 11), assimilation efficiency (F, n = 4–7), and food efficiency (G, n = 5) in HFD-fed Ppp3r1^{MlcCre} WT and KO mice.

(H) Adipocyte size (left panel) and numbers (right panel) were assessed on H&E-stained slices of epididymal white adipose tissue from HFD-fed Ppp3r1^{MlcCre} WT and KO mice (H, n = 4–7).

(I and J) Glucose tolerance tests (I) and insulin tolerance tests (J) in HFD-fed Ppp3r1^{MlcCre} WT and KO mice (n = 4–5).

(K–M) Plasma triglyceride (K), free fatty acid (L, n = 5), and plasma cholesterol (M, n = 5) levels in HFD-fed Ppp3r1^{MlcCre} WT and KO mice (n = 5).

(N) Oil red stainings of liver cryosections from HFD-fed Ppp3r1^{MlcCre} WT and KO mice.

Means ± SEM. *p < 0.05, **p < 0.01.

translated their ingested calories into body weight gain, food efficiency in Ppp3r1^{MlcCre} KO mice was poor (Figure 4G; p = 0.0084).

Muscle-specific ablation of calcineurin also led to systemic metabolic improvements, illustrated by a profoundly decreased ratio of large to small adipocytes in epididymal fat (Figure 4H, left panel) and an overall increased number of fat cells per fat pad (Figure 4H, right panel) in Ppp3r1^{MlcCre} KO mice relative to WT littermates. Preserved glucose tolerance and insulin sensitivity (Figures 4I and 4J) was paralleled by lower fasting triglyceride levels (Figure 4K) in HFD-fed Ppp3r1^{MlcCre} KO mice. Free fatty acid levels tended to be increased in HFD-fed Ppp3r1^{MlcCre} KO mice (p = 0.0811; Figure 4L), but similar respiratory quotients (Figure S3L) indicate that there is no overt nutrient preference toward burning lipids or glucose between the genotypes. Cholesterol levels remained unchanged (Figure 4M). Moreover, Ppp3r1^{MlcCre} KO mice displayed a profound protection from diet-induced steatohepatitis, as observed by lower levels of oil red staining in liver cryosections (Figure 4N).

Gene Enrichment Analyses from Skeletal Muscle of Global and Tissue-Specific Loss-Of-Function Mice Reflect a Critical Role for Calcineurin in Maintaining Metabolic Homeostasis

To identify the gene-regulatory programs that coordinate metabolic changes in skeletal muscle of calcineurin-deficient mice, we conducted whole-genome microarrays of gastrocnemii from HFD-fed Ppp3cb WT and KO mice as well as from HFD-fed Ppp3r1^{MlcCre} WT and KO mice. A heatmap analysis (Figure S3M) revealed highly similar gene deregulations in skeletal muscle of global and skeletal muscle-specific KO mice compared to their corresponding WT controls, confirming shared mechanistic underpinnings for the phenotypes of both genetic models (GEO series identifier GSE71174). Subsequent gene enrichment analyses revealed the overrepresentation of genes and pathways critical for metabolic homeostasis (Figure S3N; Table S3), and corroborated several metabolic traits observed in vivo in calcineurin KO mice.

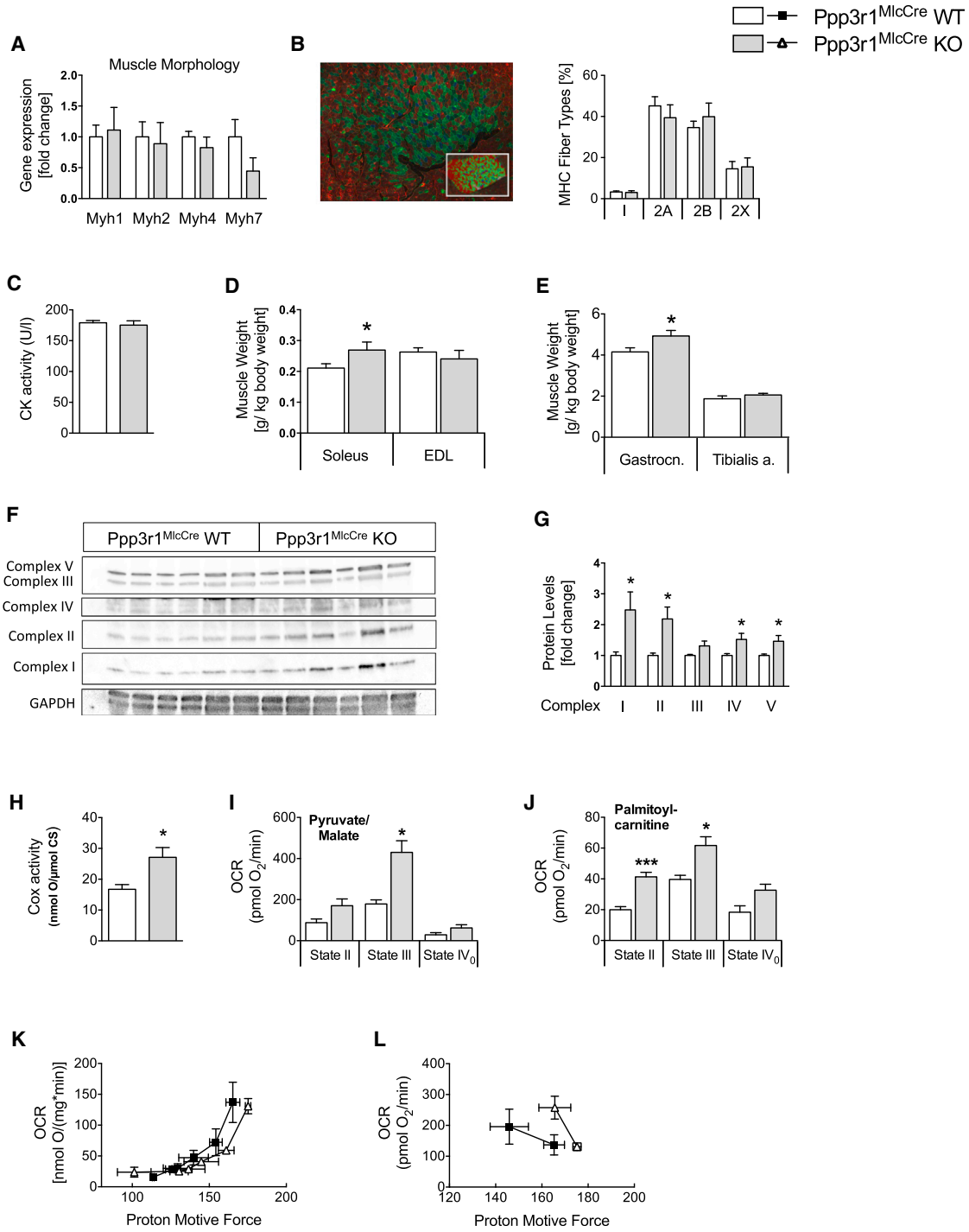

Figure 5. Inconspicuous Muscle Morphology but Increased Mitochondrial Respiration in HFD-Fed Male Ppp3r1^{MlcCre} KO Mice

(A) Myosin heavy-chain 1, 2, 4, and 7 expression in the gastrocnemius muscle of HFD-fed Ppp3r1^{MlcCre} WT and KO mice (n = 4)

(B) Immunohistochemical staining of gastrocnemius fiber types (B) and automated fiber type analyses (n = 8; inlet and right panel) of HFD-fed Ppp3r1^{MlcCre} WT and KO mice. Muscle fiber types include slow myosin oxidative fibers (blue color), MHC 2A fast oxidative fibers (green color cytosolic), and MHC 2B fast glycolytic fibers (red color cytosolic). Dystrophin staining (green color membrane) indicates cell membranes.

(C–E) Plasma creatine kinase levels (C, n = 7–14) and weights for the tibialis anterior, extensor digitorum longus (EDL), soleus and gastrocnemius of HFD-fed Ppp3r1^{MlcCre} WT and KO mice (D and E, n = 8–14; normalized to body weight).

(F and G) Western blots and densitometric analyses (n = 6) of electron transport chain complex proteins I–V in gastrocnemius muscle of HFD-fed Ppp3r1^{MlcCre} WT and KO mice.

(H) Polarographic measurement of COX activity normalized to citrate synthase activity in gastrocnemius homogenates of HFD-fed Ppp3r1^{MlcCre} WT and KO mice (n = 5–6)

(legend continued on next page)

HFD Exposure Impedes Calcineurin Expression in Skeletal Muscle

We next exposed young male C57Bl6J mice to chow or HFD to explore the impact of the dietary environment on calcineurin activity in skeletal muscle. *Ppp3cb* and *Ppp3r1* gene expression was decreased in the gastrocnemius of HFD fed-mice, compared to chow-fed controls (Figures S4A and S4B). We further observed a simultaneous increase in both *CAIN* gene expression (Figure S4C) and protein levels (Figures S4D and S4E) in the gastrocnemius but not soleus after 1 week of HFD feeding, compared to chow controls. Prolonged HFD exposure for 19 weeks had no further effects on CAIN protein levels (Figures S4D and S4E).

Calcineurin Ablation Increases Skeletal Muscle Mass and NOR-1 Expression

We next aimed to assess whether calcineurin deficiency affects mitochondrial morphology and function. While we did not find differences in gastrocnemius fiber type composition (Figures 5A and 5B) or creatine kinase activity (Figure 5C), we did observe increased muscle weight (soleus and gastrocnemius, normalized to body weight) in HFD-fed Ppp3r1^{MlcCre} KO mice compared to WT littermates (Figures 5D and 5E). We also found increased levels of myogenin (Figure S4F), a myoblast differentiation factor (Hasty et al., 1993) that has recently been shown to induce a shift from glycolytic to oxidative metabolism in adult muscle without affecting fiber type (Hughes et al., 1999). Interestingly, however, we did not observe changes in the expression of master regulators for mitochondrial biogenesis and muscle morphology, i.e., estrogen-related receptor alpha (*ESRR*α), GA repeat binding protein (*Gabp*α), nuclear respiratory factor 1 (*Nrf1*), peroxisome proliferator-activated receptor gamma coactivator 1-alpha (*PGC1*α), or peroxisome proliferator-activated receptor delta (*PPAR*δ), between HFD-fed Ppp3r1^{MlcCre} WT and KO mice (Figure S4G). Also, we did not find changes in the expression of key mitochondrial components of the oxidative phosphorylation cascade (Figure S4H). Gene expression of neuron-derived orphan receptor 1 (*NOR-1*) was elevated in gastrocnemii of HFD-fed KO mice compared to WT mice (Figure S4I). Nor-1 controls oxidative metabolism in skeletal muscle (Pearen et al., 2008), and mice with skeletal muscle-specific Nor-1 overexpressor mice are protected from DIO (Pearen et al., 2012). *NOR-1* overexpression in mice has recently been shown to increase the overall oxidative capacity of skeletal muscle (Pearen et al., 2008; 2013), prompting us to explore mitochondrial respiration in more detail.

Muscle-Specific Calcineurin Ablation Enhances Mitochondrial Electron Transfer Protein Levels, COX Activity, ATP-Coupled Respiration, and Substrate Oxidation Kinetics

In gastrocnemii of HFD-fed Ppp3r1^{MlcCre} mice, we observed increased protein levels of OXPHOS complexes I, II, IV, and V and a strong trend ($p = 0.062$) toward increased complex III protein levels, compared to HFD-fed WT controls (Figures 5F and 5G). Polarographic analyses further revealed elevated complex IV (cytochrome *c* oxidase, COX) activity in gastrocnemius homogenates of HFD-fed Ppp3r1^{MlcCre} KO mice (Figure 5H). Ppp3r1^{MlcCre} KO mice further displayed increased state 2 respiration and ATP-coupled respiration (state 3) as well as a strong trend toward increased proton leak respiration (state 4o) in mitochondrial isolates, using pyruvate/malate as electron donor to complex I (Figure 5I). Similarly, using palmitoyl-carnitine as an electron donor to electron-transfer-flavoprotein (ETF), we observed strong trends for state 2 and 4o respiration and significantly increased state 3 ATP-coupled respiration (Figure 5J). The titration of oxygen consumption rates (OCR) versus membrane potential (proton motive force) further revealed unchanged proton leak kinetics (Figure 5K), but increased substrate oxidation kinetics (Figure 5L) in HFD-fed Ppp3r1^{MlcCre} KO mice.

Ablation of Calcineurin Enhances Drp1 Serine 637-Mediated Mitochondrial Elongation

Calcineurin dephosphorylates the inhibitory serine 637 residue of Drp1, thereby facilitating translocation of Drp1 to mitochondria (Cereghetti et al., 2008, 2010; Cribbs and Strack, 2007). Accordingly, we hypothesized that calcineurin ablation would lead to Ser637-Drp1 hyperphosphorylation and a shift toward mitochondrial fusion (Figure 6A).

Overall protein levels of OPA1 and mitofusin, key regulators of mitochondrial fusion, as well as Drp1, key mediator of fission, were similar between genotypes in gastrocnemius muscle of HFD-fed Ppp3r1^{MlcCre} WT and KO mice (Figure 6B). However, in HFD-fed Ppp3r1^{MlcCre} KO mice we observed Drp1 hyperphosphorylation at serine 637 (= serine 600 in mice). Drp1 phosphorylation at Ser637 was also induced in C2C12 myotubes treated overnight with calcineurin inhibitor FK-506 and protein kinase A activator forskolin (Figure S5A). Coincubation of C2C12 myotubes with serum from mice fed either chow or HFD—but not fatty acids alone—could aggravate the synergistic effect of FK-506 and forskolin on Ser637-Drp1 hyperphosphorylation (Figures S5B and S5C).

Consistent with the known impact of Drp1 Ser637 hyperphosphorylation on mitochondrial elongation, we discovered enhanced mitochondrial elongation in skeletal muscle of Ppp3r1^{MlcCre} KO mice (Figure 6C) and in C2C12 cells with Drp1^{Ser637} mutations (Figure S5D). Transmission electron microscopy (TEM) of soleus muscle from HFD-fed Ppp3r1^{MlcCre} WT and KO mice revealed numerous fusion events in the KO mice (Figure 6C, indicated by arrows). We next corroborated our finding of enhanced mitochondrial fusion using calcineurin mutant flies. TEM of indirect flight muscles of the mutants *dCanA1* or *dCanA-14F* specifically showed increased fusion and elongated mitochondrial filaments (Figure 6D, indicated by arrows).

(I and J) Oxygen consumption rates (OCR) in isolated mitochondria of gastrocnemius from HFD-fed Ppp3r1^{MlcCre} WT and KO mice (n = 3). Measurements were conducted with an extracellular flux analyzer (Seahorse Bioscience) using pyruvate/malate (I) and palmitoylcarnitine (J) as substrates.

(K and L) Titration of OCRs to the proton motive force revealed no evidence for changes in proton leak kinetics (K, n = 3) but increased substrate oxidation kinetics (L, n = 3) in Ppp3r1^{MlcCre} KO mice.

Means ± SEM. *$p < 0.05$, ***$p < 0.001$.

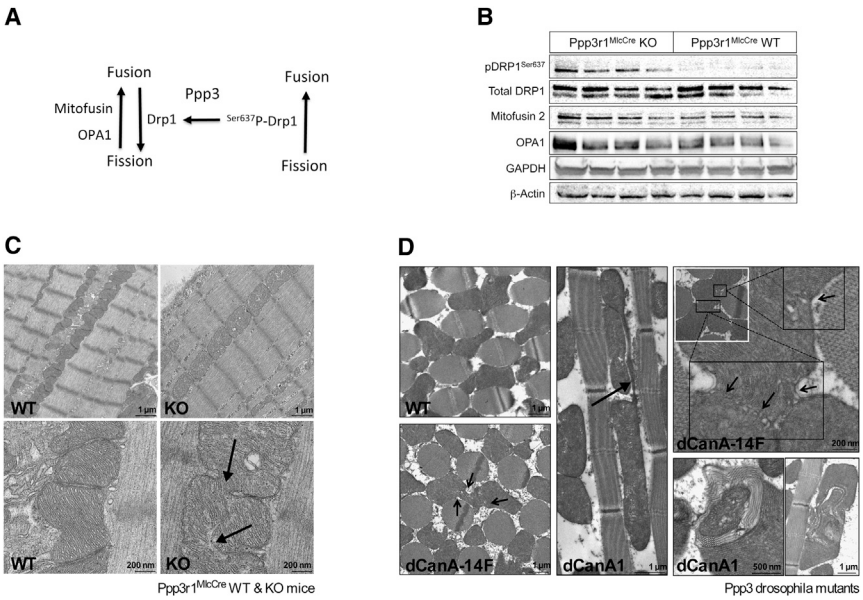

Figure 6. Ablation of *Ppp3* in Muscle Induces Drp1-Ser^{637} Hyperphosphorylation and Mitochondrial Elongation

(A) Regulation of mitochondrial fission-fusion-dynamics by calcineurin.

(B) Western blot analyses of key components of the mitochondrial dynamics machinery reveal Ser637 hyperphosphorylation of Drp1 in male Ppp3r1^{MlcCre} KO mice.

(C and D) Transmission electron microscopy (TEM) from soleus of male Ppp3r1^{MlcCre} WT and KO mice (C), and from indirect flight muscle of male *Drosophila* calcineurin mutants *dCNA-14F* and *dCanA1*. Fusion events are indicated by black arrows.

Calcineurin Deficiency Promotes Exercise-Induced Mitochondrial Filament Elongation in Skeletal Muscle

Exercise is well known for its extensive remodeling of skeletal muscle (Egan and Zierath, 2013), partly mediated via calcineurin (Long and Zierath, 2008). We here aimed to assess whether moderate exercise could also differentially affect calcineurin-driven mitochondrial dynamics. TEM revealed the formation of long mitochondrial filaments in the soleus and gastrocnemius (Figures 7A–7E) of exercised Ppp3cb KO mice. Subsarcolemmal mitochondrial elongation in the soleus seemed to be directed toward the intramyofibrillar space (indicated by arrows), elongation of fibers spanning the intermyofibrillar space occurred close to the Z-disc (indicated by stars). Notably, subsarcolemmal mitochondria in the soleus of Ppp3cb KO mice appear elongated already in the sedentary state, compared to WT controls (Figure 7C). In the gastrocnemius, exercise-induced mitochondrial elongation occurred solely in Ppp3cb KO mice and was located in the I-band close to the Z-disc (Figure 7B, indicated by arrows).

Full Calcineurin Ablation Attenuates Exercise Performance

The discovery of a role for calcineurin in the impact that exercise has on mitochondrial morphology and function in muscle led us to evaluate the physical performance of Ppp3cb KO mice during a strenuous exercise challenge. HFD-fed Ppp3cb WT and KO mice displayed similar treadmill performance with unchanged overall running distance or work capacity (Figure 7F). In contrast, when subjected to the same strenuous exercise, Ppp3r1^{MlcCre} KO mice reached exhaustion with a shorter overall running distance and lower overall work capacity compared to WT controls (Figure 7G). Nevertheless, despite a severely diminished treadmill performance, HFD-fed Ppp3r1^{MlcCre} KO mice displayed unconstrained locomotor activity in their home cage, as revealed by an infrared beam break system (Figure 7H).

DISCUSSION

We provide evidence that serine threonine phosphatase calcineurin acts as environmentally controlled regulator of mitochondrial dynamics and systemic energy and body weight homeostasis. Fly mutants revealed alterations in body weight, metabolic rates, triacylglycerol, and glycogen stores. Global Ppp3cb KO mice revealed a congruent phenotype including diminished fat mass; protection from body weight gain; and alterations in food intake, feed efficiency, and energy expenditure. Our finding of full protection from DIO and its sequelæ in mice with conditional ablation of Ppp3r1 from skeletal muscle—but not from adipose tissue or liver—validates an essential and highly conserved role for skeletal muscle calcineurin in metabolic control.

Protection from DIO has been reported previously for a murine model of skeletal muscle-specific overexpression of activated calcineurin (Jiang et al., 2010). The fact that calcineurin overexpression evokes a similar metabolic phenotype as its knockout seems counterintuitive but might be based on the finding that calcineurin overexpression induces a massive switch toward red, oxidative type 1 fibers (Jiang et al., 2010; Naya et al., 2000). Such a profound switch toward oxidative red fibers results in increased mitochondrial biogenesis and respiration and systemically elevated energy expenditure and has been reported for skeletal muscle-specific PPARdelta (Wang et al., 2004) and *PGC1α* (Lin et al., 2002) overexpressor mice. Calcineurin overexpression in cardiac muscle was further shown to induce superoxide production and mitochondrial dysfunction, ultimately leading to cardiac failure (Sayen et al., 2003). Notably, we did not observe any switch in fiber types or pathological changes in muscle morphology, as evidenced by inconspicuous muscle ultrastructure and unaffected creatine kinase levels, in our muscle-specific Ppp3r1 KO mice. Overall, our fly and mouse models of calcineurin deficiency seem to reflect a physiological state without adverse superoxide production where murine skeletal muscle is mostly comprised of white, glycolytic type 2 fibers.

Calcineurin can dephosphorylate pro-fission dynamin related protein 1 (Drp1) at Ser 637, thereby inducing Drp1 translocation to the mitochondrial membrane and mitochondrial fission (Cereghetti et al., 2008, 2010). In humans, calcineurin activation was associated with changes in skeletal muscle mitochondrial

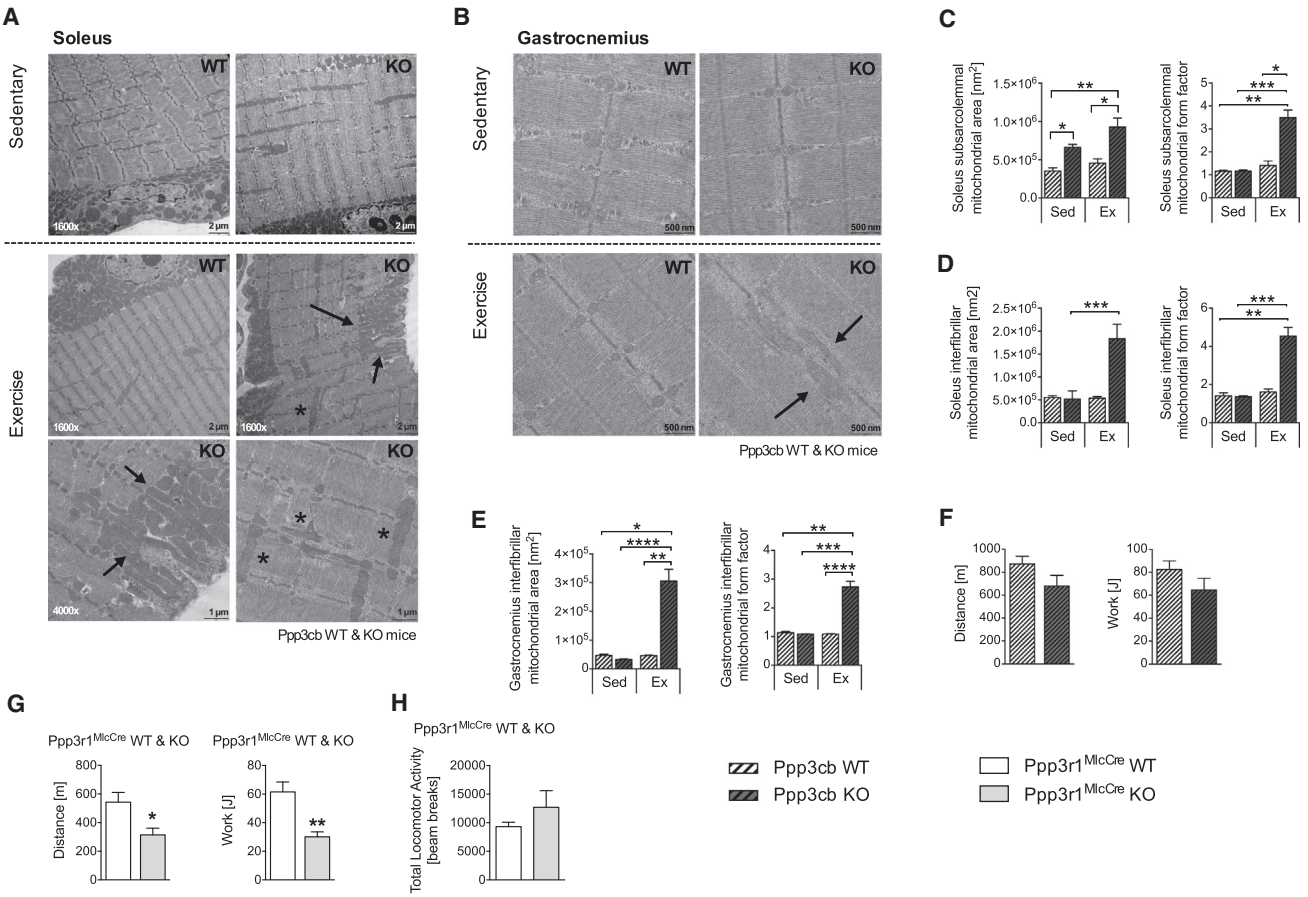

Figure 7. Exercise-Induced Mitochondrial Elongation and Exercise Capacity in Male Calcineurin Mutant Mice

(A and B) TEM from soleus (A) and gastrocnemius muscles (B) of chow-fed Ppp3cb WT and KO mice after moderate, nonexhaustive treadmill exercise (3 hr, 5° inclination, maximum speed 17 m/s). Stars (A) or arrows (B) indicate elongated mitochondrial filaments spanning the intermyofibrillar space and elongated fibers close to the Z-disc. Arrows in (A) indicate filament elongation of subsarcolemmal mitochondria.

(C–E) Quantification of elongated mitochondrial areas (left panel) and form factors (right panel) for soleus subsarcolemmal (C) and interfibrillar (D), and gastrocnemius interfibrillar (E) mitochondria of exercised Ppp3cb WT and KO mice (n = 6–9).

(F and G) Exhaustion treadmill performance test (20° inclination, 5 m/min for 4 min, 14 m/min for 2 min, incremental increase by 2 m/min every 2 min until mice reach exhaustion) in HFD-fed Ppp3cb WT and KO mice (F, n = 9) and HFD-fed Ppp3r1^{MIcCre} WT and KO mice (G, n = 9–15).

(H) Unconstrained home cage activity of HFD-fed Ppp3r1^{MIcCre} WT and KO mice was assessed by an infrared beam break system (n = 5).

Means ± SEM. *p < 0.05, **p < 0.01.

dynamics (Garnier et al., 2005). An exercise intervention trial in obese insulin-resistant adults further suggested that decreased activation of Drp1 upon exercise may facilitate lifestyle-mediated improvements in substrate metabolism and insulin sensitivity (Fealy et al., 2014). A recent report revealed that chronic HFD exposure can impede mitochondrial fusion and disrupt the dynamic remodeling of an extended filamentous network of mitochondrial nanotubules in skeletal muscle of mice (Liu et al., 2014). Our data of increased inhibitory Drp1^{Ser637} phosphorylation and a shift toward mitochondrial elongation in calcineurin mutant flies and mice are in line with the peer-reviewed literature and identify calcineurin as a physiological mediator of such mitochondrial elongation. Our finding of increased gene and protein expression of calcineurin inhibitor *CAIN* (Lai et al., 1998) following 1 week of HFD exposure further suggests that a transient decrease of calcineurin activity may be a physiologically relevant compensatory mechanism by skeletal muscle to prevent detrimental effects of HFD exposure on mitochondrial dynamics.

The existence of elongated filaments and power cable-shaped mitochondrial clusters that span sarcomeres and the intramyofibrillar space had been suggested before by Vladimir Skulchev (Skulachev, 2001), who hypothesized that such mitochondrial filaments would complement damaged mitochondria and serve as an effective power transmission system between remote parts of the cell. Elongated mitochondria were further shown to possess more cristae and increased ATP synthase activity (Gomes et al., 2011), which is in line with our finding of increased complex 4 activity and mitochondrial respiration in gastrocnemius of HFD-fed Ppp3r1^{MIcCre} KO mice.

Notably, in Ppp3cb KO mouse muscle undergoing moderate treadmill exercise, we also observed a shift in orientation of subsarcolemmal mitochondria to form filaments that permeate into the intramyofibrillar space. Intramyofibrillar mitochondria

are enriched with adenine nucleotide translocase, which augments the exchange of mitochondrial ATP for cytosolic ADP and thus coupling and efficiency (Roussel et al., 2000). However, intramyofibrillar mitochondria suffer from limited oxygen supply, which represents a rate-limiting step for ATP production. Subsarcolemmal mitochondria may display limited coupling efficiency and ATP production compared to intramyofibrillar mitochondria (Mollica et al., 2006), but their close proximity to the vasculature ensures a rich oxygen supply and the constant regeneration of proton motive force. Overall, our electron microscopy findings in calcineurin mutant flies and mice support a model whereby enhanced fusion, elongated filaments, and reorientation of the mitochondrial network can facilitate the power transmission of a proton gradient between oxygen-rich subsarcolemmal mitochondria and oxygen-deprived intramyofibrillar mitochondria to increase oxidative energy metabolism.

Remodeling of mitochondrial membrane interactions in mouse muscle after acute exercise had been shown before (Picard et al., 2013), but the molecular mechanisms remained elusive. We propose here that calcineurin may represent an environmental sensor that governs mitochondrial dynamics to augment oxidative metabolism along the myofiber in times of energy demand. However, we also show impaired exercise capacity in HFD-fed Ppp3r1^{MlcCre} KO mice. Exhaustive exercise was shown to induce excessive oxygen radical formation (Davies et al., 1982) in muscle and mitochondrial fission in myotubes (Fan et al., 2010). Fragmentation of mitochondria provides an important quality control mechanism to maintain bioenergetics efficiency by sequestering and eliminating damaged mitochondria via autophagy (Twig et al., 2008). Blocking mitochondrial fission is detrimental when cells undergo excessive environmental stress, and has been linked with lethality upon full inhibition (Ishihara et al., 2009; Waterham et al., 2007). Our finding of unchanged exhaustive exercise capacity in Ppp3cb mutants further suggests that the remaining catalytic subunits *Ppp3ca* and *Ppp3cc* can partially compensate for the loss of *Ppp3cb*, and retain some phosphatase activity toward Drp1 and the control of mitochondrial fusion-fission dynamics. In contrast, full ablation of calcineurin activity and impaired exhaustive exercise capacity in Ppp3r1^{MlcCre} KO mice are further evidence that mitochondrial fission is critical for cellular homeostasis when environmental stress exceeds a yet-to-be-defined threshold.

Immunosuppression therapy by high-dose treatment with calcineurin inhibitors cylosporin A or tacrolimus (FK-506) has been associated with a higher prevalence for developing obesity and diabetes in patients. However, the literature is conflicting, and both weight gain and weight loss are reported (Toulson Davisson Correia et al., 2003). Potential drug interactions, often-severe side effects, and the progressed disease state of patients render it nearly impossible to draw clear conclusion on direct effects of calcineurin inhibitors for body weight and glucose control. For instance, concomitant adrenal corticosteroid therapy may explain the observed weight gain in some patients (Palmer et al., 1991), and tacrolimus seems to excert less weight gain compared to cyclosporin A (López-Vilella et al., 2015; Mor et al., 1995; Neal et al., 2001). A recent patent application suggests the use of very low doses of tacrolimus or close structural analogs to prevent fat accumulation and sarcopenia in elderly patients (Akoulitchev et al., 2014). Currently, clinical data on low-dose calcineurin inhibition in humans are not available, but rodent studies using low-dose FK-506 treatment (1 mg/kg/day) show a (reversible) reduction of body weight gain (Ishida et al., 1997), which is in line with our own data. Accordingly, low-dose calcineurin inhibitors may indeed have beneficial health effects and may hold direct translational relevance for the treatment of obesity in patients.

In conclusion, we reveal an evolutionarily conserved role for skeletal muscle calcineurin in the adaptive regulation of body weight and energy homeostasis. Our data suggest calcineurin activity is a critical determinant for the environmental control of mitochondrial elongation via Drp1^{Ser637} dephosphorylation in skeletal muscle. Ablation of calcineurin in flies and mice leads to the formation of power-cable-shaped mitochondrial filaments within muscle fibers, which may optimize the efficiency for oxidative phosphorylation. Nevertheless, impaired exhaustive exercise capacity in Ppp3r1 mutants suggests that intact mitochondrial fission-fusion-dynamics are essential for an adequate adaptive response upon excessive environmental stress.

EXPERIMENTAL PROCEDURES

Fly Studies

D. melanogaster piggyBac transposon insertion mutants (Thibault et al., 2004) (PBac{WH}CanA1[f01787] [Calcineurin A1] and PBac{WH}CanA-14F[f02374] [CanA at 14-F]) and the isogenic wild-type w^{1118} strain (BL-6326) were ordered from Exelixis *Drosophila* Stock Collection at Harvard Medical School and subjected to metabolic characterization as described (De Luca et al., 2005; Jumbo-Lucioni et al., 2010). For detailed information see Supplemental Experimental Procedures.

Mouse Studies

Generation of Ppp3cb (calcineurin A beta) knockout mice and double-fluorescent mG/mT Cre reporter mice has been described previously (Bueno et al., 2002a, 2002b; Muzumdar et al., 2007). Conditional Ppp3r1 (Ppp3r1$^{fl/fl}$) mice (Neilson et al., 2004) were crossed to adiponectin (Wang et al., 2010), albumin (Postic et al., 1999), or myosin light-chain 1f (Bothe et al., 2000) Cre mice. For detailed information see Supplemental Experimental Procedures.

Histology and Transmission Electron Microscopy

Tricolor stainings of myosin heavy-chain (MHC) isoforms, liver oil red staining of frozen hepatic sections, hematoxylin & eosin (H&E) staining of paraffin-embedded tissue, fluorescence microscopy of Mlc1f-driven Cre recombination in double fluorescent Cre reporter, and TEM of fixed skeletal muscle sections are decribed in the Supplemental Experimental Procedures.

Body Composition and Indirect Calorimetry

Fat mass and lean mass were assessed using NMR technology (EchoMRI, Houston, TX, USA). Food intake, energy expenditure, respiratory quotients, and locomotor activity were measured using a combined indirect calorimetry system (TSE Systems GmBH, Bad Homburg, Germany), as described (Pfluger et al., 2008). Mice had free access to food and water and were adapted to the cages for 24–72 hr.

Western Blotting

Proteins were detected using standard procedures with antibodies directed against Drp1 (mouse monoclonal, 1:1,000, BD Biosciences), phospho-Drp1S637 (rabbit monoclonal, 1:1,000, Cell Signaling), Opa1 (mouse monoclonal 1:1,000, BD Biosciences), mitofusin2 (rabbit monoclonal, 1:1,000, Abcam), Anti-Rt/Ms Total OxPhos Complex Kit (mouse monoclonal antibody cocktail, 1:2,000, Invitrogen), CAIN (rabbit polyclonal, 1:1,000, Abcam), GAPDH (mouse monoclonal, 1:20,000, Santa Cruz Biotechnologies), and β-actin (1:10,000, rabbit polyclonal, Cell Signaling Technology).

Real-Time Gene Expression and Gene Array Analyses

RNA was isolated and transcribed using standard procedures. Gene expression was analyzed using taqman probes (Applied Biosystems, Carlsbad, CA, USA) or custom-made primers (Sigma, St. Louis, MO, USA) with *HPRT* or *RPL32* as housekeeping genes. For mouse microarray analyses, equal amounts of RNA were submitted to the Cincinnati Children's Hospital Medical Center (CCHMC) gene expression core facility for Affymetrix Gene 1.0 ST Array analyses (Affymetrix, Santa Clara, CA, USA). Gene enrichment analyses were performed using the web-based ToppGene Suite interface (Chen et al., 2009).

Mitochondrial Respiration in Skeletal Muscle

A detailed description on the isolation of mitochondria and measurement of mitochondrial respiration is given in the Supplemental Experimental Procedures.

Adiabatic Bomb Calorimetry

Adiabatic bomb calorimetry was performed as described (Olszewski et al., 2012). Briefly, food consumption was monitored in single-housed mice for 5–7 days, and feces collected. Energy contents of the dried and pelleted samples were measured in a bomb calorimeter (IKA Calorimeter C7000, Staufen, Germany). Energy assimilation efficiencies were calculated from ingested food energy versus egested feces energy.

Glucose, Pyruvate, and Insulin Tolerance Tests

Mice were subjected to 6 hr of fasting and injected ip with 2 g glucose/kg body weight for the GTT, and 0.75 or 1.0 U insulin/kg body weight (Humolog, Lily, Indianapolis, USA) for the ITT. For the PTT, mice were fasted for 16 hr and subjected to 2 g pyruvate/kg body weight. Tail blood glucose levels (mg/dL) were measured using a handheld glucometer (TheraSense Freestyle) before (0 min) and at 15, 30, 60, and 120 min after injection. Glucose-stimulated insulin secretion was assessed in overnight-fasted mice by injection of 2 g glucose/kg body weight using blood collected from the tail.

Plasma Parameters

Plasma insulin, leptin, adiponectin, resistin, and tPAI-1 levels were measured by xMAP-based multiplex technology (Luminex, St. Charles, Missouri, USA). Insulin secretion was assessed with an ultra-sensitive mouse insulin ELISA (ChrystalChem, Downers Grove, IL, USA). Tyroxine levels were measured by a radioimmunoassay (DSL, Webster, TX, USA). Plasma creatine kinase activity, glucose, and nonesterified fatty acid (NEFA) levels were measured using enzymatic kits (BioAssay Systems, Hayward, CA, USA; Autokit Glucose, and NEFA C, Wako, Neuss, Germany). Plasma cholesterol and triglyceride levels were determined using Infinity Cholesterol or Infinity Triglyceride reagent, respectively (Thermo Electron, Pittsburgh, PA, USA).

Statistical Analysis

Statistical analyses were performed using GraphPad Prism 6 (GraphPad Software, Inc. La Jolla, CA, USA) or SPSS (IBM, Armonk, NY, USA). Differences between phenotypes were assessed using untailed Student's t tests, or one-way or two-way ANOVA with Bonferroni's post test, as indicated. Differences in energy expenditure were assessed by Analysis of Co-Variance (ANCOVA) using body weight as covariate. Electron microscopy results were assessed by using nonparametric Kruskal-Wallis one-way ANOVA with Dunn's multiple comparison post tests. p values lower than 0.05 were considered significant. All results are presented as means ± SEM.

SUPPLEMENTAL INFORMATION

Supplemental Information includes five figures, three tables, and Supplemental Experimental Procedures and can be found with this article at http://dx.doi.org/10.1016/j.cmet.2015.08.022.

ACKNOWLEDGMENTS

We thank Marlene Kilian, Gayathri Anantakrishnan, Cynthia Striese, Nilika Chaudhary, Jazzminn Hembree, and Nickki Ottaway for technical assistance and Silke Morin for language editing of the manuscript. P.T.P., D.G.K., K.P., S.C.S., V.C.G., T.D.M., and D.P.-T. performed experiments in mice; J.W., S.M.R., and M.D.L. performed experiments in flies. J.R. and M.H.d.A. conducted the bomb calorimetry. M.L., M.A., A.F., and A.W. evaluated tissue histology; M.K. and M.J. assessed mitochondrial respiration. B.J.A. assessed microarray data; P.T.P., J.E., A.L.H., J.D.M., and M.H.T. conceptualized all experiments and interpreted the results. P.T.P. and M.H.T. wrote the manuscript. This work was supported by funding from the Alexander von Humboldt Foundation, the Deutsches Zentrum für Diabetesforschung (DZD), the Helmholtz Portfolio Theme Metabolic Dysfunction and Common Disease, and the Helmholtz Alliance ICEMED—Imaging and Curing Environmental Metabolic Diseases.

Received: January 27, 2015
Revised: May 13, 2015
Accepted: August 25, 2015
Published: September 24, 2015

REFERENCES

Akoulitchev, A., Milway, E., Mellor, E.J., and Youdell, M. (2014). Tacrolimus and analogues thereof for medical use. Patent application WO2014188198 A1.

Bothe, G.W., Haspel, J.A., Smith, C.L., Wiener, H.H., and Burden, S.J. (2000). Selective expression of Cre recombinase in skeletal muscle fibers. Genesis *26*, 165–166.

Bueno, O.F., Brandt, E.B., Rothenberg, M.E., and Molkentin, J.D. (2002a). Defective T cell development and function in calcineurin A beta -deficient mice. Proc. Natl. Acad. Sci. USA *99*, 9398–9403.

Bueno, O.F., Wilkins, B.J., Tymitz, K.M., Glascock, B.J., Kimball, T.F., Lorenz, J.N., and Molkentin, J.D. (2002b). Impaired cardiac hypertrophic response in Calcineurin Abeta -deficient mice. Proc. Natl. Acad. Sci. USA *99*, 4586–4591.

Cereghetti, G.M., Stangherlin, A., Martins de Brito, O., Chang, C.R., Blackstone, C., Bernardi, P., and Scorrano, L. (2008). Dephosphorylation by calcineurin regulates translocation of Drp1 to mitochondria. Proc. Natl. Acad. Sci. USA *105*, 15803–15808.

Cereghetti, G.M., Costa, V., and Scorrano, L. (2010). Inhibition of Drp1-dependent mitochondrial fragmentation and apoptosis by a polypeptide antagonist of calcineurin. Cell Death Differ. *17*, 1785–1794.

Chen, J., Bardes, E.E., Aronow, B.J., and Jegga, A.G. (2009). ToppGene Suite for gene list enrichment analysis and candidate gene prioritization. Nucleic Acids Res. *37*, W305–W311.

Cribbs, J.T., and Strack, S. (2007). Reversible phosphorylation of Drp1 by cyclic AMP-dependent protein kinase and calcineurin regulates mitochondrial fission and cell death. EMBO Rep. *8*, 939–944.

Davies, K.J., Quintanilha, A.T., Brooks, G.A., and Packer, L. (1982). Free radicals and tissue damage produced by exercise. Biochem. Biophys. Res. Commun. *107*, 1198–1205.

De Luca, M., Yi, N., Allison, D.B., Leips, J., and Ruden, D.M. (2005). Mapping quantitative trait loci affecting variation in Drosophila triacylglycerol storage. Obes. Res. *13*, 1596–1605.

Dietrich, M.O., Antunes, C., Geliang, G., Liu, Z.-W., Borok, E., Nie, Y., Xu, A.W., Souza, D.O., Gao, Q., Diano, S., et al. (2010). Agrp neurons mediate Sirt1's action on the melanocortin system and energy balance: roles for Sirt1 in neuronal firing and synaptic plasticity. J. Neurosci. *30*, 11815–11825.

Egan, B., and Zierath, J.R. (2013). Exercise metabolism and the molecular regulation of skeletal muscle adaptation. Cell Metab. *17*, 162–184.

Fan, X., Hussien, R., and Brooks, G.A. (2010). H2O2-induced mitochondrial fragmentation in C2C12 myocytes. Free Radic. Biol. Med. *49*, 1646–1654.

Fealy, C.E., Mulya, A., Lai, N., and Kirwan, J.P. (2014). Exercise training decreases activation of the mitochondrial fission protein dynamin-related protein-1 in insulin-resistant human skeletal muscle. J. Appl. Physiol. *117*, 239–245.

Garnier, A., Fortin, D., Zoll, J., N'Guessan, B., Mettauer, B., Lampert, E., Veksler, V., and Ventura-Clapier, R. (2005). Coordinated changes in mitochondrial function and biogenesis in healthy and diseased human skeletal muscle. FASEB J. *19*, 43–52.

Gomes, L.C., Di Benedetto, G., and Scorrano, L. (2011). During autophagy mitochondria elongate, are spared from degradation and sustain cell viability. Nat. Cell Biol. *13*, 589–598.

Hasty, P., Bradley, A., Morris, J.H., Edmondson, D.G., Venuti, J.M., Olson, E.N., and Klein, W.H. (1993). Muscle deficiency and neonatal death in mice with a targeted mutation in the myogenin gene. Nature *364*, 501–506.

Hughes, S.M., Chi, M.M., Lowry, O.H., and Gundersen, K. (1999). Myogenin induces a shift of enzyme activity from glycolytic to oxidative metabolism in muscles of transgenic mice. J. Cell Biol. *145*, 633–642.

Ishida, H., Mitamura, T., Takahashi, Y., Hisatomi, A., Fukuhara, Y., Murato, K., and Ohara, K. (1997). Cataract development induced by repeated oral dosing with FK506 (tacrolimus) in adult rats. Toxicology *123*, 167–175.

Ishihara, N., Nomura, M., Jofuku, A., Kato, H., Suzuki, S.O., Masuda, K., Otera, H., Nakanishi, Y., Nonaka, I., Goto, Y., et al. (2009). Mitochondrial fission factor Drp1 is essential for embryonic development and synapse formation in mice. Nat. Cell Biol. *11*, 958–966.

Jiang, B., and Cyert, M.S. (1999). Identification of a novel region critical for calcineurin function in vivo and in vitro. J. Biol. Chem. *274*, 18543–18551.

Jiang, L.Q., Garcia-Roves, P.M., de Castro Barbosa, T., and Zierath, J.R. (2010). Constitutively active calcineurin in skeletal muscle increases endurance performance and mitochondrial respiratory capacity. Am. J. Physiol. Endocrinol. Metab. *298*, E8–E16.

Jumbo-Lucioni, P., Ayroles, J.F., Chambers, M.M., Jordan, K.W., Leips, J., Mackay, T.F., and De Luca, M. (2010). Systems genetics analysis of body weight and energy metabolism traits in Drosophila melanogaster. BMC Genomics *11*, 297.

Klee, C.B., Crouch, T.H., and Krinks, M.H. (1979). Calcineurin: a calcium- and calmodulin-binding protein of the nervous system. Proc. Natl. Acad. Sci. USA *76*, 6270–6273.

Klettner, A., and Herdegen, T. (2003). FK506 and its analogs—therapeutic potential for neurological disorders. Curr. Drug Targets CNS Neurol. Disord. *2*, 153–162.

Lai, M.M., Burnett, P.E., Wolosker, H., Blackshaw, S., and Snyder, S.H. (1998). Cain, a novel physiologic protein inhibitor of calcineurin. J. Biol. Chem. *273*, 18325–18331.

Lee, D., Le Lay, J., and Kaestner, K.H. (2014). The transcription factor CREB has no non-redundant functions in hepatic glucose metabolism in mice. Diabetologia *57*, 1242–1248.

Liesa, M., and Shirihai, O.S. (2013). Mitochondrial dynamics in the regulation of nutrient utilization and energy expenditure. Cell Metab. *17*, 491–506.

Liesa, M., Palacín, M., and Zorzano, A. (2009). Mitochondrial dynamics in mammalian health and disease. Physiol. Rev. *89*, 799–845.

Lin, J., Wu, H., Tarr, P.T., Zhang, C.-Y., Wu, Z., Boss, O., Michael, L.F., Puigserver, P., Isotani, E., Olson, E.N., et al. (2002). Transcriptional co-activator PGC-1 alpha drives the formation of slow-twitch muscle fibres. Nature *418*, 797–801.

Liu, L., Zhang, J., Yuan, J., Dang, Y., Yang, C., Chen, X., Xu, J., and Yu, L. (2005). Characterization of a human regulatory subunit of protein phosphatase 3 gene (PPP3RL) expressed specifically in testis. Mol. Biol. Rep. *32*, 41–45.

Liu, R., Jin, P., Yu, L., Wang, Y., Han, L., Shi, T., and Li, X. (2014). Impaired mitochondrial dynamics and bioenergetics in diabetic skeletal muscle. PLoS ONE *9*, e92810.

Long, Y.C., and Zierath, J.R. (2008). Influence of AMP-activated protein kinase and calcineurin on metabolic networks in skeletal muscle. Am. J. Physiol. Endocrinol. Metab. *295*, E545–E552.

López-Vilella, R., Sánchez-Lázaro, I.J., Martínez-Dolz, L., Almenar-Bonet, L., Marqués-Sulé, E., Melero-Ferrer, J., Portolés-Sanz, M., Rivera-Otero, M., Domingo-Valero, D., and Montero-Argudo, A. (2015). Incidence of development of obesity after heart transplantation according to the calcineurin inhibitor. Transplant. Proc. *47*, 127–129.

Mollica, M.P., Lionetti, L., Crescenzo, R., D'Andrea, E., Ferraro, M., Liverini, G., and Iossa, S. (2006). Heterogeneous bioenergetic behaviour of subsarcolemmal and intermyofibrillar mitochondria in fed and fasted rats. Cell. Mol. Life Sci. *63*, 358–366.

Mor, E., Facklam, D., Hasse, J., Sheiner, P., Emre, S., Schwartz, M., and Miller, C. (1995). Weight gain and lipid profile changes in liver transplant recipients: long-term results of the American FK506 Multicenter Study. Transplant. Proc. *27*, 1126.

Muzumdar, M.D., Tasic, B., Miyamichi, K., Li, L., and Luo, L. (2007). A global double-fluorescent Cre reporter mouse. Genesis *45*, 593–605.

Naya, F.J., Mercer, B., Shelton, J., Richardson, J.A., Williams, R.S., and Olson, E.N. (2000). Stimulation of slow skeletal muscle fiber gene expression by calcineurin in vivo. J. Biol. Chem. *275*, 4545–4548.

Neal, D.A., Gimson, A.E., Gibbs, P., and Alexander, G.J. (2001). Beneficial effects of converting liver transplant recipients from cyclosporine to tacrolimus on blood pressure, serum lipids, and weight. Liver Transpl. *7*, 533–539.

Neilson, J.R., Winslow, M.M., Hur, E.M., and Crabtree, G.R. (2004). Calcineurin B1 is essential for positive but not negative selection during thymocyte development. Immunity *20*, 255–266.

Olszewski, P.K., Rozman, J., Jacobsson, J.A., Rathkolb, B., Strömberg, S., Hans, W., Klockars, A., Alsiö, J., Risérus, U., Becker, L., et al. (2012). Neurobeachin, a regulator of synaptic protein targeting, is associated with body fat mass and feeding behavior in mice and body-mass index in humans. PLoS Genet. *8*, e1002568.

Palmer, M., Schaffner, F., and Thung, S.N. (1991). Excessive weight gain after liver transplantation. Transplantation *51*, 797–800.

Pearen, M.A., Myers, S.A., Raichur, S., Ryall, J.G., Lynch, G.S., and Muscat, G.E.O. (2008). The orphan nuclear receptor, NOR-1, a target of β-adrenergic signaling, regulates gene expression that controls oxidative metabolism in skeletal muscle. Endocrinology *149*, 2853–2865.

Pearen, M.A., Eriksson, N.A., Fitzsimmons, R.L., Goode, J.M., Martel, N., Andrikopoulos, S., and Muscat, G.E.O. (2012). The nuclear receptor, Nor-1, markedly increases type II oxidative muscle fibers and resistance to fatigue. Mol. Endocrinol. *26*, 372–384.

Pearen, M.A., Goode, J.M., Fitzsimmons, R.L., Eriksson, N.A., Thomas, G.P., Cowin, G.J., Wang, S.C.M., Tuong, Z.K., and Muscat, G.E.O. (2013). Transgenic muscle-specific Nor-1 expression regulates multiple pathways that effect adiposity, metabolism, and endurance. Mol. Endocrinol. *27*, 1897–1917.

Pfluger, P.T., Herranz, D., Velasco-Miguel, S., Serrano, M., and Tschöp, M.H. (2008). Sirt1 protects against high-fat diet-induced metabolic damage. Proc. Natl. Acad. Sci. USA *105*, 9793–9798.

Picard, M., Gentil, B.J., McManus, M.J., White, K., St Louis, K., Gartside, S.E., Wallace, D.C., and Turnbull, D.M. (2013). Acute exercise remodels mitochondrial membrane interactions in mouse skeletal muscle. J. Appl. Physiol. *115*, 1562–1571.

Postic, C., Shiota, M., Niswender, K.D., Jetton, T.L., Chen, Y., Moates, J.M., Shelton, K.D., Lindner, J., Cherrington, A.D., and Magnuson, M.A. (1999). Dual roles for glucokinase in glucose homeostasis as determined by liver and pancreatic beta cell-specific gene knock-outs using Cre recombinase. J. Biol. Chem. *274*, 305–315.

Reddy, P.H., Reddy, T.P., Manczak, M., Calkins, M.J., Shirendeb, U., and Mao, P. (2011). Dynamin-related protein 1 and mitochondrial fragmentation in neurodegenerative diseases. Brain Res. Brain Res. Rev. *67*, 103–118.

Roussel, D., Chainier, F., Rouanet, J., and Barré, H. (2000). Increase in the adenine nucleotide translocase content of duckling subsarcolemmal mitochondria during cold acclimation. FEBS Lett. *477*, 141–144.

Rusnak, F., and Mertz, P. (2000). Calcineurin: form and function. Physiol. Rev. *80*, 1483–1521.

Sayen, M.R., Gustafsson, A.B., Sussman, M.A., Molkentin, J.D., and Gottlieb, R.A. (2003). Calcineurin transgenic mice have mitochondrial dysfunction and elevated superoxide production. Am. J. Physiol. Cell Physiol. *284*, C562–C570.

Schneeberger, M., Dietrich, M.O., Sebastián, D., Imbernón, M., Castaño, C., Garcia, A., Esteban, Y., Gonzalez-Franquesa, A., Rodríguez, I.C., Bortolozzi, A., et al. (2013). Mitofusin 2 in POMC neurons connects ER stress with leptin resistance and energy imbalance. Cell *155*, 172–187.

Skulachev, V.P. (2001). Mitochondrial filaments and clusters as intracellular power-transmitting cables. Trends Biochem. Sci. *26*, 23–29.

Suk, H.Y., Zhou, C., Yang, T.T.C., Zhu, H., Yu, R.Y.L., Olabisi, O., Yang, X., Brancho, D., Kim, J.-Y., Scherer, P.E., et al. (2013). Ablation of calcineurin Aβ reveals hyperlipidemia and signaling cross-talks with phosphodiesterases. J. Biol. Chem. *288*, 3477–3488.

Thibault, S.T., Singer, M.A., Miyazaki, W.Y., Milash, B., Dompe, N.A., Singh, C.M., Buchholz, R., Demsky, M., Fawcett, R., Francis-Lang, H.L., et al. (2004). A complementary transposon tool kit for Drosophila melanogaster using P and piggyBac. Nat. Genet. *36*, 283–287.

Toulson Davisson Correia, M.I., Rego, L.O., and Lima, A.S. (2003). Post-liver transplant obesity and diabetes. Curr. Opin. Clin. Nutr. Metab. Care *6*, 457–460.

Tschöp, M.H., Speakman, J.R., Arch, J.R.S., Auwerx, J., Brüning, J.C., Chan, L., Eckel, R.H., Farese, R.V., Jr., Galgani, J.E., Hambly, C., et al. (2012). A guide to analysis of mouse energy metabolism. Nat. Methods *9*, 57–63.

Twig, G., Hyde, B., and Shirihai, O.S. (2008). Mitochondrial fusion, fission and autophagy as a quality control axis: the bioenergetic view. Bioenergetics *1777*, 1092–1097.

Wang, Y.-X., Zhang, C.L., Yu, R.T., Cho, H.K., Nelson, M.C., Bayuga-Ocampo, C.R., Ham, J., Kang, H., and Evans, R.M. (2004). Regulation of muscle fiber type and running endurance by PPARdelta. PLoS Biol. *2*, e294.

Wang, Z.V., Deng, Y., Wang, Q.A., Sun, K., and Scherer, P.E. (2010). Identification and characterization of a promoter cassette conferring adipocyte-specific gene expression. Endocrinology *151*, 2933–2939.

Wang, Y., Li, G., Goode, J., Paz, J.C., Ouyang, K., Screaton, R., Fischer, W.H., Chen, J., Tabas, I., and Montminy, M. (2012). Inositol-1,4,5-trisphosphate receptor regulates hepatic gluconeogenesis in fasting and diabetes. Nature *485*, 128–132.

Waterham, H.R., Koster, J., van Roermund, C.W.T., Mooyer, P.A.W., Wanders, R.J.A., and Leonard, J.V. (2007). A lethal defect of mitochondrial and peroxisomal fission. N. Engl. J. Med. *356*, 1736–1741.